

# System-Level Simulation of 120 kW Interior Permanent Magnet Synchronous Motor Drive for Electric Vehicle Usage Under Various Types of Faults for Fault Diagnosis

Woyeong Kwon<sup>1</sup>, Jaewook Oh<sup>1</sup>, Inhyeok Hwang<sup>1</sup>, Bowook Choi<sup>2</sup>, and Namsu Kim<sup>1\*</sup>

<sup>1</sup>*Department of Mechanical and Aerospace Engineering, Konkuk University, 120 Neungdong-ro, Gwangji-gu, Seoul, Republic of Korea, 05029*

*woyeong@naver.com  
jhow93@konkuk.ac.kr  
dlsgur5560@naver.com  
nkim7@konkuk.ac.kr*

<sup>2</sup>*Defense System Management Team, Hyundai Rotem, 37 Cheoldobangmulgwan-ro, Uiwang-si, Gyeonggi-do, Republic of Korea, 16082*

*bwchoi@hyundai-rotam.co.kr*

## ABSTRACT

Owing to the recent trend toward the zero-carbon emission, drive motors are gaining attention for substitute for internal combustion engine. Among them, interior permanent magnet synchronous motor(IPMSM) is being extensively used for their high-power density. Consequently, verification of safety and reliability for IPMSM is becoming an important subject. In this study, system-level simulation for IPMSM drive system under various failure modes were carried out. Fault characteristics were extracted from the phase current profile and classified by the support vector machine. It is shown that with the proposed model, faults can be detected with less cost and time-consumption.

## 1. INTRODUCTION

Recently, there has been a growing trend towards zero-carbon emissions in the automotive industry, leading to increased interest in electric drive motors as a substitute for internal combustion engines(ICEs). Among the various types of electric drive motors, interior permanent magnet synchronous motor(IPMSM) is one of the most widely used types due to their numerous advantages including high-power density. As a consequence, ensuring the safety and reliability of IPMSM have become an important research subject. To address this need, failure modes and effect analysis(FMEA) must be carried out. However, it is costly and time-consuming to manufacture test motors for multiple failure modes. System-level motor drive simulations can be

a cost-effective and time-efficient alternative to conducting real experiments. They can provide data that are closely resembles real-world scenarios. Due to these advantages, many studies have been conducted using simulations to diagnose the possible failure modes in IPMSM. Stanely, Henk, and Jan (2007) designed a radial-flux outer-rotor PMSM. N. A. Al-Nuaim and Humid (1997) modeled a PMSM to diagnose the eccentricity fault. J. Farooq, S. Srairi, Abdesslem, and abdellatif (2006) modeled an outer-rotor PMSM under demagnetization for fault diagnosis.

In this paper, a system-level simulation model of a 120 kW IPMSM drive was modeled to diagnose static eccentricity(SE), dynamic eccentricity(DE), mixed eccentricity(ME), and demagnetization(DM) faults. The healthy motor's flux linkage map considering the geometry of the motor was constructed using a finite element analysis(FEA). Then, the flux linkage map was converted into a three-dimensional look-up table(LUT). The conversion process utilized inverse calculations instead of derivatives to reduce computational time. The LUT was linked with the motor control unit(MCU) consisting of controllers and a space vector pulse width modulation(SVPWM) inverter. For the MCU, two modeling methods, current-state variable model(CSVM) and flux-state variable model(FSVM) were employed to compare the performance. To validate the simulation model, experiment using the healthy motor was conducted. Based on the validated model, SE, DE, ME, and DM faults were implemented, and fault-related frequency components were extracted from the phase current data. Finally, support vector machine(SVM) was used for diagnosing and classifying the faults.

First Author et al. This is an open-access article distributed under the terms of the Creative Commons Attribution 3.0 United States License, which permits unrestricted use, distribution, and reproduction in any medium, provided the original author and source are credited.

The remainder of this paper is composed as follows: Section 2 explains the backgrounds for the failure modes. Section 3 presents the modeling methods of the motors and MCU. Section 4 shows the experimental setup and validation results. Section 5 demonstrates the classification results. Finally, section 6 concludes this paper.

## 2. BACKGROUND FOR FAILURE MODES

### 2.1. Eccentricity

Eccentricity fault refers to the misalignment of the center of stator and rotor. They can be classified into three types, static, dynamic, and mixed, according to the state of the misalignment. If the center of the stator is misaligned with the center of rotor and rotation, it is classified as SE. Else if the center of the rotor is misaligned with the center of the stator and rotation, it is called DE. The ME is the coexistence of SE and DE. Under eccentricity fault, the air gap between the stator and rotor becomes non-uniformly distributed. The non-uniform distribution of the air gap induces unbalanced magnetic pull(UMP). The UMP generates additional torque pulsations, which results in increased noise and vibration. Bashir, Jawad, and Mehrsan (2009) found that due to the nature of the rotating machinery, certain sideband harmonics increase under eccentricity fault, which can be calculated as:

$$f_{eccen} = \frac{2k-1}{P} \cdot f_1 \quad (1)$$

where,  $f_{eccen}$  is the fault characteristic frequency of eccentricity,  $k$  is the positive integer,  $P$  is the number of pole pairs, and  $f_1$  is the fundamental frequency.

### 2.2. Demagnetization

The coercivity force, which refers to the ability of the magnet to endure external magnetic field without being demagnetized, decreases under high temperature. The IPMSMs in electric vehicles operate in a wide speed and torque range. During high-speed or high-torque operation, the operating temperature increases due to the high current input and vibrations. In this case, the permanent magnets(PMs) in the rotor can be easily demagnetized. Under DM, controller increases the input current to maintain constant torque output under decreased PM magnetic flux. If the PMs are partially demagnetized, certain fault characteristic frequency components will increase. However, if the PMs are uniformly demagnetized, there are no significant change in frequency domain except for the rise in the fundamental frequency and its harmonics.

## 3. MODELING METHOD

### 3.1. Current-State Variable Method

From the study by Sebastian, Fabien, Johan, and Claudia (2019), the voltage and torque equations of the CSVM method can be stated as follows :

$$V_d = L_d \frac{di_d}{dt} + R_s i_d - \omega_e L_q i_q \quad (2)$$

$$V_q = L_d \frac{di_q}{dt} + R_s i_q + \omega_e (\Psi_m + L_d i_d) \quad (3)$$

$$T_{em} = \frac{3p}{2} [\Psi_m i_q + (L_d - L_q) i_d i_q] \quad (4)$$

where,  $V_d$  and  $V_q$  are the d- and q-axis voltage,  $L_d$  and  $L_q$  are the d- and q-axis inductance,  $i_d$  and  $i_q$  are the d- and q-axis current,  $R_s$  is the stator resistance,  $\Psi_m$  is the flux linkage of the PM,  $\omega_e$  is the angular speed in electrical degrees,  $p$  is the number of pole pairs, and  $T_{em}$  is the electromagnetic torque. In the CSVM model,  $L_d, L_q$ , and  $\Psi_m$  are the functions of  $i_d$  and  $i_q$ . This method cannot consider the effect of motor topology. In addition, the model includes derivatives computations, which can provoke numerical instabilities. To deal with this problem, electromagnetic torque data was extracted from the FEA. The derivatives of the torque data were converted to the LUT and linked with the simulation loop.

### 3.2. Flux-State Variable Method

From the study done by Sebastian et al. (2019), the voltage and torque equations in FSVM can be stated as follows:

$$V_d = \frac{d\Psi_d}{dt} + R_s i_d - \omega_s \Psi_q \quad (5)$$

$$V_q = \frac{d\Psi_q}{dt} + R_s i_q - \omega_s \Psi_d \quad (6)$$

$$\Psi_d = f(i_d, i_q, \theta) \quad (7)$$

$$\Psi_q = g(i_d, i_q, \theta) \quad (8)$$

$$T_{em} = \frac{mp}{2} [\Psi_d i_q - \Psi_q i_d] \quad (9)$$

where,  $\Psi_d$  and  $\Psi_q$  are the d- and q-axis flux linkage. Since the flux linkage components are the functions of  $i_d, i_q$ , and  $\theta$ , the effect of motor topology can be considered in the simulation. In addition, the time-consuming derivative calculations are substituted by inverse calculations, which can be stated as:

$$\Psi_d = \int (V_d - R_s i_d + \omega_e \Psi_q) dt \quad (10)$$

$$\Psi_q = \int (V_q - R_s i_q - \omega_e \Psi_d) dt \quad (11)$$

$$i_d = f^{-1}(\Psi_d, \Psi_q, \theta) \quad (12)$$

$$\Psi_q = g^{-1}(\Psi_d, \Psi_q, \theta) \quad (13)$$

$$T_{em} = T(i_d, i_q, \theta) \quad (14)$$

The variations of the d- and q-axis flux linkages and the torques as functions of dq currents and rotor position are obtained from the FEA.

### 3.3. Finite Element Analysis

Fig. 2 shows the cross-section of the simulated motor. The simulation was carried out by using Ansys Maxwell tool. Detailed specifications of the simulated motors are listed in Table 1. Healthy and faulty models were designed and the corresponding electromagnetic parameters were extracted and linked with the MCU model. The eccentricity faults were implemented by adjusting the centerlines of the rotor, stator, and rotation. The uniform demagnetization faults were implemented by reducing the coercivity of the PMs.

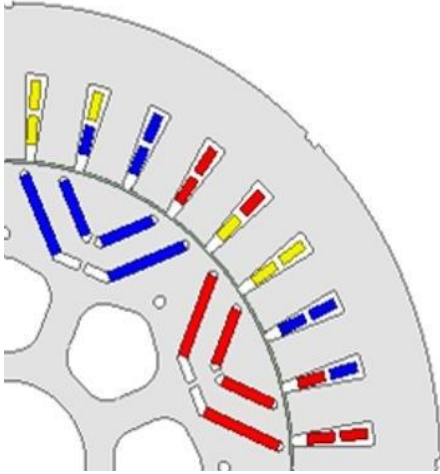


Figure 1. Cross section of the simulated motor.  
Table 1. Specifications of the simulated motor

Parameter	Unit	Value
Peak torque	<i>Nm</i>	500
Peak power	<i>kW</i>	120
Base speed	<i>rpm</i>	4360
DC link voltage	<i>V</i>	538
Max current	<i>A</i>	630
Number of pole pairs	-	4
Number of slots	-	36
Active stack length	<i>mm</i>	120
Rotor outer diameter	<i>mm</i>	210
Stator outer diameter	<i>mm</i>	320
Air gap length	<i>mm</i>	1

### 3.4. Motor Control Unit

Fig. 2 shows the schematic diagram of the MCU. A closed-loop control consisting of speed controller, current controller, and SVPWM inverter was used.

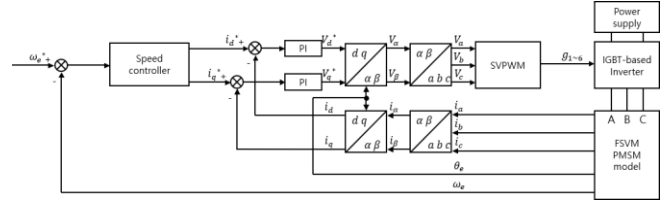


Figure 2. Block diagram of the motor control unit

### 4. EXPERIMENTAL SETUP AND VALIDATION

Fig. 3 shows the experimental setup. The 120 kW 8-pole 36-slot IPMSM was used. The 200 kW dynamometer was used to control the motor. The phase current data was obtained from the NI-9215 data acquisition setup (DAQ) from the inverter. The sampling frequency of the DAQ was set to 10 kHz.

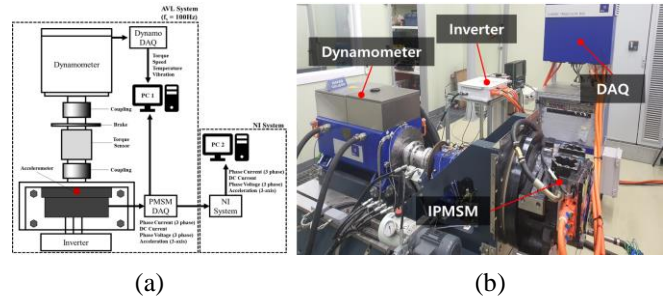


Figure 3. Experimental Setup: (a) Schematic and (b) picture.

Fig. 4 shows the phase current comparison of the CSVM, FSVM, and experimental result. As shown, the FSVM model showed more similar results with the experimental results than CSVM model.

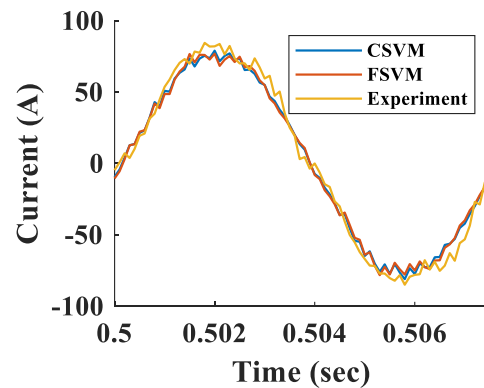


Figure 4. Phase current comparison of the CSVM and FSVM model with the experimental results. The operating speed was set to 2000 rpm, and the load torque was set to 50 Nm.

## 5. RESULT AND DISCUSSION

From the simulation data of the phase currents, fault features were extracted. For the eccentricity, fault characteristic frequencies, which are 0.25th, 0.75th, 1.25th, and 1.75th harmonics for the simulated motor, were used. For the uniform demagnetization, fundamental frequency, and its harmonics from 2nd to 8th were used. Fig. 5 shows the classification results. As can be seen, the failure modes were successfully classified.

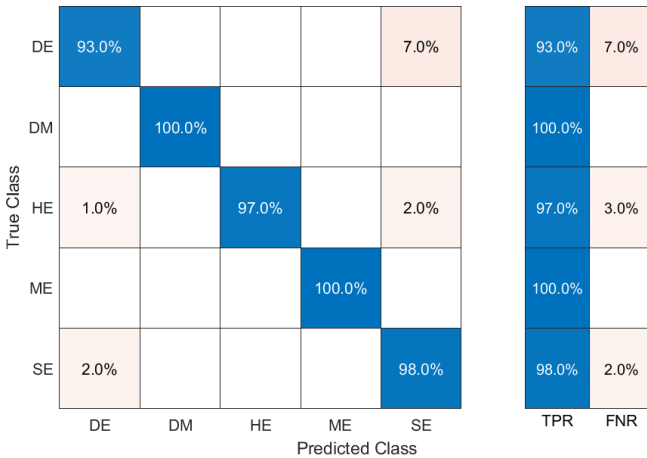


Figure 5. Confusion matrix for classification results of the failure modes.

## 6. CONCLUSION

In this paper, system-level IPMSM drive model was designed for diagnosing SE, DE, ME, and DM faults. Two different modeling methods, CSVM and FSVM, were compared. The electromagnetic parameters of the healthy motor were extracted from the FEA model. The parameters were linked with the MCU model in the form of LUT. The model was verified with the experimental results. Based on the verified model, failure modes were implemented. The phase current datasets for each failure modes were acquired. Fault features were extracted from the frequency domain of the phase current datasets and classified by using the SVM. The results shows that the proposed method can successfully classify different failure modes with relatively low cost and time-consumption.

## ACKNOWLEDGEMENT

This work was supported by Korea Research Institute for defense Technology planning and advancement(KRIT) - Grant funded by Defense Acquisition Program Administration (DAPA) (KRIT-CT-22-081, Weapon System CBM+ Research Center)

## REFERENCES

Al-Nuaim, N. A., & Toliyat, H. A., (1997). A method for dynamic simulation and detection of dynamic air-gap

eccentricity in synchronous machines. In *1997 IEEE International Electric Machines and Drives Conference Record*. doi: 10.1109/IEMDC.1997.604067

Ciceo, S., Chauvicourt, F., Gyselinck, J., & Martis, C. (2019) A comparative study of system-level PMSM models with either current or flux-linkage state variables used for vibro-acoustic computation. In *2019 IEEE International Electric Machines & Drives conference (IEMDC)*, (pp. 1881-1888). doi: 10.1109/IEMDC.2019.8785326

Ebrahimi, B. M., Faiz, J., & Roshtkhari, M. J. (2009). Static-, Dynamic-, and Mixed-Eccentricity Fault Diagnoses in Permanent-Magnet Synchronous Motors. *IEEE Transactions on Industrial Electronics*, 56(11), 4727-4739. doi: 10.1109/TIE.2009.2029577

Farooq, J., Srairi, S., Djerdir, A., & Miraoui, A. (2006). Use of permeance network method in the demagnetization phenomenon modeling in a permanent magnet motor. *IEEE Transactions on Magnetics*, 42(4), 1295-1298. doi: 10.1109/TMAG.2006.870936

Holm, S. R., Polinder, H., & Ferreira, J. A. (2007). Analytical Modeling of a Permanent-Magnet Synchronous Machine in a Flywheel. *IEEE Transactions on Magnetics*, 43(5), 1955-1967. doi: 10.1109/TMAG.2007.892791

**Woyeong Kwon** Woyeong Kwon received the B.E. degree in Department of Mechanical Engineering from Konkuk University, Seoul, Republic of Korea in 2021. He is conducting research about prognostics and health management for electrified traction system at Reliability based design optimization laboratory of Konkuk University.

**Jaewook Oh** Jaewook Oh received a B.S. degree and M.S. degree in Mechanical Engineering from Konkuk University, Seoul, Republic of Korea, in 2020 and 2022, respectively. His current research focus is on prognostics and health management of traction electric motors and DC-AC traction inverters.

**Inhyeok Hwang** Inhyeok Hwang received a B.S. degree and M.S. degree in Mechanical Engineering from Konkuk University, Seoul, Republic of Korea, in 2020 and 2022, respectively. His current research focus is on prognostics and health management for electric motors.

**Namsu Kim** Namsu Kim received the B.E. degree in mechanical engineering from Hanyang University in 1998, the M.S. degree in mechanical engineering from the University of Texas at Austin in 2005, and the Ph.D. degree in mechanical engineering from the Georgia Institute of Technology in 2009. From 2010 to 2015, he was a Senior Researcher with the Korea Electronics Technology Institute. He is currently an Associate Professor of Mechanical Engineering with Konkuk University, Seoul, South Korea. His current research focus on design optimization including

prognostics and health management of mechanical and electrical component.